Supporting Information

Anisotropic Nano-sheets Self-assembly to Impede Charge Injection into Polymer Dielectrics

Ying Zhou[1‡], Anna M. LaChance[2,3‡], Qian Wang[1‡], Yanfeng Gao[4‡], Jierui Zhou[5,6], Bangdou Huang[7], Kuangyu Shen[2,3], Zaili Hou[2,3], Ting Lei[1], Ningzhen Wang[8], Zhou Zuo[1], Shan Liu[9], Leonard A. Dissado[10], Tao Shao[7], Xidong Liang[1], Yang Cao[5,6**], Luyi Sun[2,3***], Chao Wu[1****]*

1. Methods

Preparation of PVA-MMT nanocoatings. As presented in Figure S1a, a polyvinyl alcohol (PVA) solution was prepared by dissolving PVA pellets in deionized (DI) water with the assistance of brief heating. MMT powders were dispersed in DI water with the assistance of stirring for 30 min followed by brief ultrasonication (Branson 8510R-MT, 250 W, 44 kHz) to ensure a uniform exfoliation. Subsequently, the PVA solution was slowly added to the MMT aqueous dispersion to achieve a total solid concentration of 1.5 wt. %, where the MMT loading fraction in the total solids was varied (e.g., for a 50 wt. % MMT loading, 0.75 wt. % MMT + 0.75 wt. % PVA + 98.5 wt. % of DI water was used). The mixture was stirred for an additional 30 min followed by a brief period of ultrasonication to ensure uniform dispersion. The surfaces of the PS films (10 μm in thickness) were pre-processed to reduce the surface energy and improve the wettability with a corona discharge treater (Electro Technic Products BD-20AC Laboratory) with a 3-inch field effect electrode (operating at 45 kV and 4.5 MHz), which was waved ca. 1.5 inches above the film in a steady uniform horizontal pattern across the entire surface on each side of the film. The PS films were dip-coated with the above-

mentioned aqueous dispersion and then vertically hung in an oven to be dried at 60 °C. The low viscosity dispersion helped to generate a quick flow and a thin liquid layer, both of which are favorable for achieving a high level of orientation of MMT nanosheets. The coating process was repeated twice, four times, six times, or eight times with the films being rotated 180° before the next cycle of dip coating to maintain an even coating layer on the substrate surface, generating coatings with a thickness of 155 ± 2 nm (twice), 324 ± 6 nm (four times), 446 ± 5 nm (six times), and 621 ± 8 nm (eight times). Flexible, transparent PS films with and without the PVA/MMT coating (50 wt. % MMT, 324 ± 6 nm) are shown in Figure S1b and S1c.

Analysis of SAXS. SAXS patterns are shown in Figure S2. The first-order Bragg peaks (θ_B) were observed from the SAXS profiles, with their intensity increasing as the φ value approaches the Bragg angle. The rocking curve is presumably symmetric with respect to $\theta = \theta_B$. The intensities at $2\theta_B$ as a function of φ, were plotted and then fit using the Lorentz distribution as follows:

$$I = I_0 + \frac{2A}{\pi}\frac{w}{4(\varphi-\theta_B)^2+w^2} \qquad \text{(S1)}$$

where I_0 is the background, A is the area under the curve, and w is the FWHM.

Measurement of space charge and electric field distortion. As shown in Figure S3, pressure pulse is generated when the pulsed laser irradiates the metal electrode on film, disturbing the chare distribution, which generated the current in external circuit. The short-circuit current is given by: [S1]

$$I_{\mathrm{sc}}(t) = -\left(2 - \frac{1}{\varepsilon_{\mathrm{r}}}\right)\chi P c^2 \tau \frac{A}{d} \backslash \rho(z), \quad \frac{d}{c} \gg \tau \qquad \text{(S2)}$$

where χ is the compressibility of film, P is the amplitude of pressure pulse, A and d are the area and thickness of film, ρ is the charge density and $z = ct$ is the space coordinate.

Then the internal electric field can be calculated by Poisson's formula, and the distortion of the electric field can be obtained further.

2. Properties

Patterns of the breakdown regions. As presented in Figure S4, the size of PS and PSMMT perforations varies in each experiment, but there are always radial traces on the surface of PSMMT film, providing the channel for charge release.

Integrated Conduction and dielectric constant. As shown in Figure S5.

Storage characteristic. The D-E hysteresis loop of PS and PSMMT is shown in Figure S6. It has been tested under 100Hz half-sinusoid. The calculated of discharged energy density and charge-discharge efficiency can be obtained using the method in Supporting information of reference. [S2]

REFERENCES

S1. Huang, B.; Yu, J.; Dong, J.; Zhou, Y.; Zhai, L.; Dou, L.; Wu, C.; Liang, X.; Zhang, C.; Ostrikov, K.; Shao, T. Improving Charge Storage of Biaxially-Oriented Polypropylene under Extreme Electric Fields by Excimer UV Irradiation. Adv. Mater. 2311713 (2024).

S2. Wu, C.; Deshmukc, A.; Yassin, O.; Zhou, J.; Alamri, A.; Vellek, J.; Shukla, S.; Sotzing, M.; Casalini, R.; Sotzing, G.; Cao, Y. Flexible cyclic-olefin with enhanced dipolar relaxation for harsh condition electrification. Proc. Natl. Acad. Sci. 118, e2115367118 (2021).

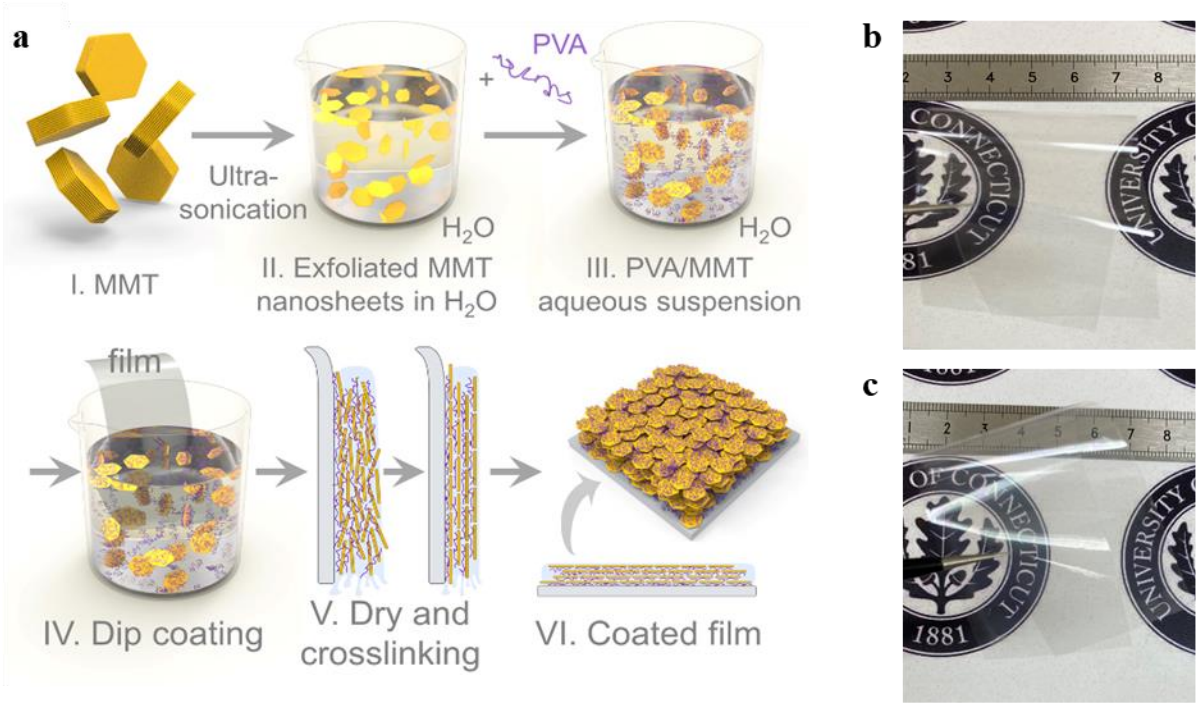

Figure S1. Preparation of PVA-MMT nanocoatings. (a) Schematic of the self-assembly coating process. Photo of (b) the uncoated and (c) PVA-MMT coated PS films.

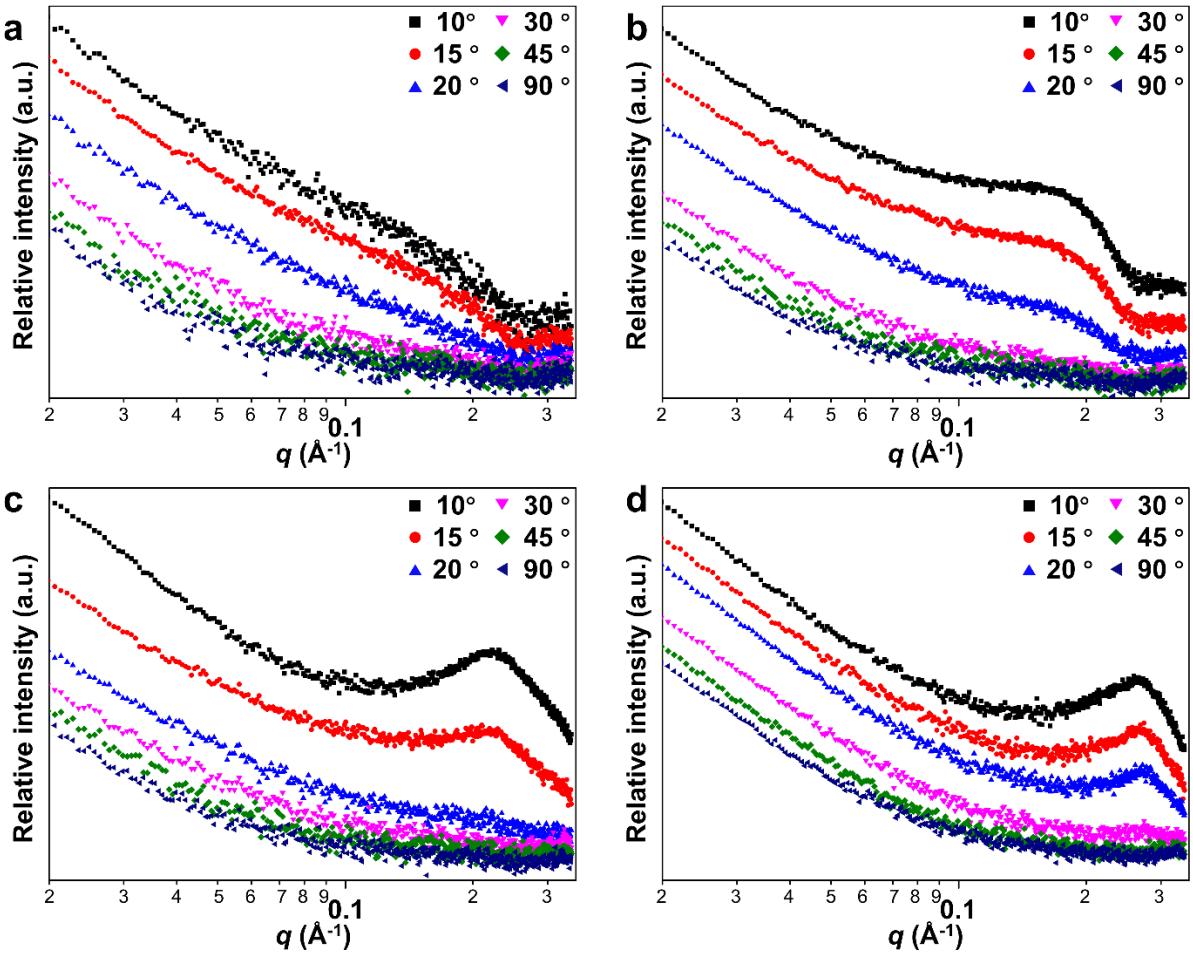

Figure S2. SAXS patterns of the 4-cycle nanocoatings containing (a) 10 wt. %, (b) 30 wt. %, (c) 50 wt. %, and (d) 65 wt. % MMT nanosheets.

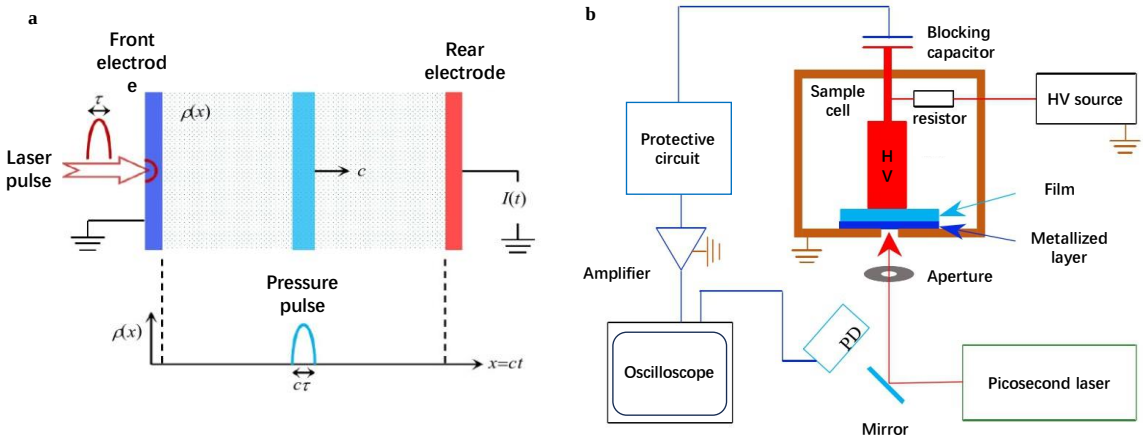

Figure S3. Measurement of high precision space charge. (a) Principle and (b) Device schematic of Laser Induced Pressure Pulse (LIPP).

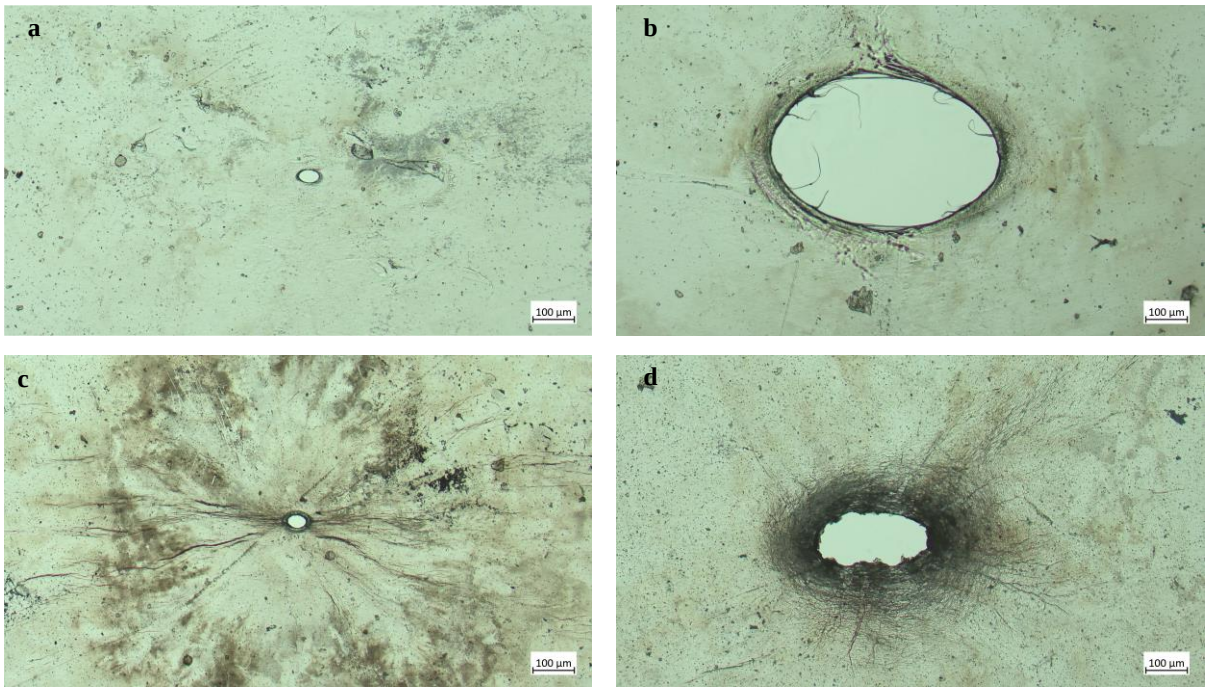

Figure S4. Patterns of the breakdown regions of (a-b) PS ans (c-d) PSMMT.

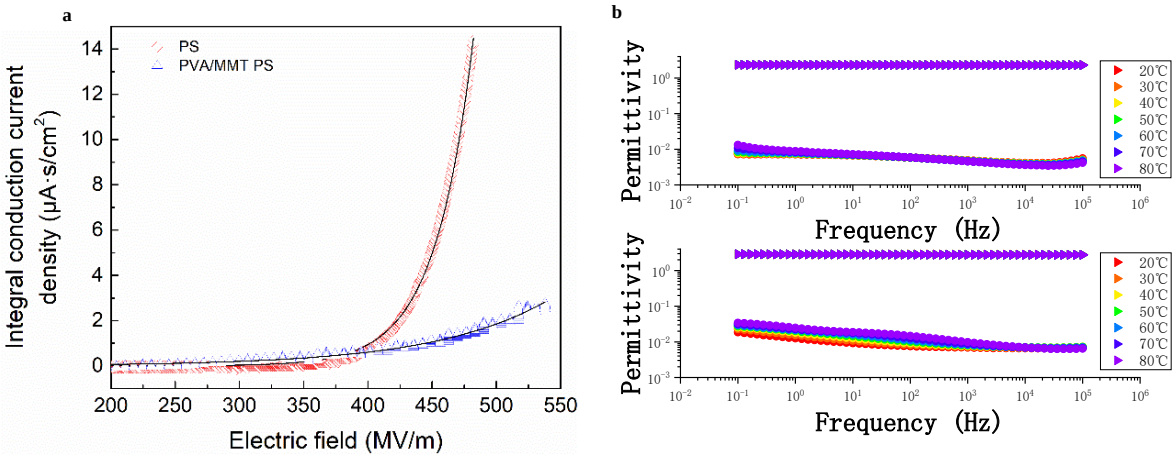

Figure S5. Some other properties of PS and PSMMT. (a) Integral conduction current density and (b) permittivity of PS and PSMMT.

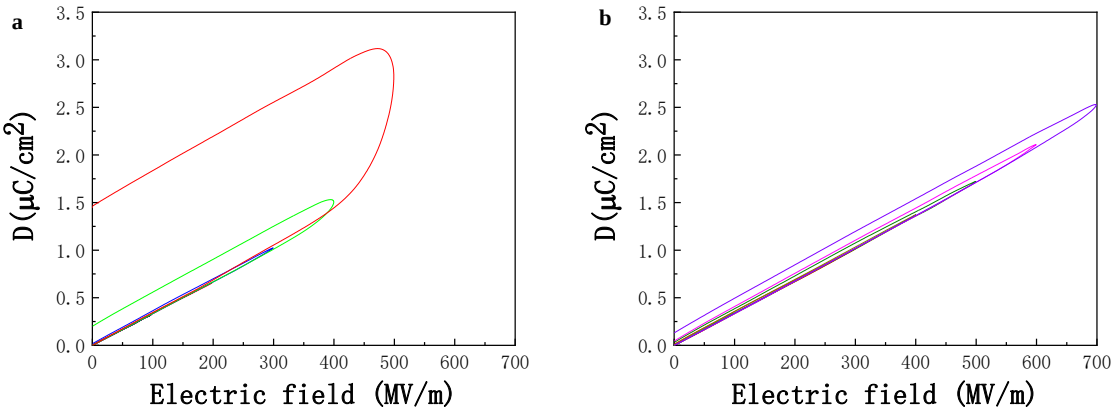

Figure S6. The D-E hysteresis loop of (a) PS and (b) PSMMT.